Journal of Wind Engineering & Industrial Aerodynamics 172 (2018) 139–151

Contents lists available at ScienceDirect

Journal of Wind Engineering & Industrial Aerodynamics

journal homepage: www.elsevier.com/locate/jweia

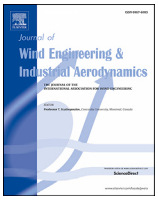

Large Eddy Simulation of an isolated vertical axis wind turbine

Antonio Posa[a,b,*], Elias Balaras[b]

[a] CNR-INSEAN, Marine Technology Research Institute, Via di Vallerano 139, 00128 Rome, Italy
[b] Department of Mechanical and Aerospace Engineering, The George Washington University, 800 22nd Street, N.W., Washington, DC, 20052, USA

ARTICLE INFO

Keywords:
Vertical axis wind turbines
Wake flow
Dynamic stall
Tip speed ratio
Large Eddy Simulation
Immersed boundary method

ABSTRACT

A computational study is presented on the wake features of a Vertical Axis Wind Turbine (VAWT), with a particular focus on the way stall phenomena lead to the formation of large coherent structures. In our earlier work (Int. J. Heat Fluid Flow 61: 75–84, 2016) numerical results were compared with experiments carried out in similar conditions. The operation of VAWTs is characterized by the generation of large vortices, especially at low Tip Speed Ratios (*TSRs*), corresponding to larger angles of attack. In the present study the use of a Large Eddy Simulation (LES) approach, coupled with an immersed-boundary (IB) formulation, allowed the solution of such coherent structures, which were found to affect substantially the flow within the rotor and downstream of the turbine. Two values of *TSR* are investigated here, in order to discuss its influence on the wake structure. Lower *TSRs* are associated to boundary layer separation closer to the leading edge of the blades and larger rollers, during both upwind and downwind stall. Upwind stall affects more substantially wake properties, producing larger structures populating the leeward side of the overall wake.

1. Introduction

During the past three decades most of the investments in wind farming have been in Horizontal Axis Wind Turbine (HAWT) technology. HAWTs are the most common technology used to convert wind to energy, with more than 90% of the market share (AWEA, 2012). These are typically large turbines (60–90 m tall) and extensive research has been done to maximize the power output of HAWTs farms (see Barthelmie and Jensen, 2010; Cal et al., 2010; for example). Wake interference is a major issue in HAWTs wind farms, where turbines need to be spaced far enough from each other to operate practically in isolation. As a consequence HAWTs require substantial land resources and are located away from urban areas, where most of the power is needed. An alternative technology are Vertical Axis Wind Turbines (VAWTs), which have seen renewed research efforts recently. Typical VAWTs have a small footprint and their generators and gearboxes are even closer to the ground for easy maintenance (see Jha, 2011). They are nearly silent and can operate at wind speeds of approximately 5 m per second. Land resources required by VAWTs are typically smaller, since in their case it is possible to increase the swept area by just increasing their height, with no additional footprint. Perhaps the biggest benefit is that VAWTs can be placed closer together, without a reduction in turbine efficiency. Field testing in a small scale VAWTs farm deployed for research purposes suggest that their wakes can be optimized by configuring turbines in counter-rotating pairs, decreasing the overall size of wind farm arrays (see Dabiri, 2011; for details). The beneficial interaction of VAWTs pairs has also been confirmed in numerical studies by Giorgetti et al. (2015), Bremseth and Duraisamy (2016), Kanner et al. (2016) and Brownstein et al. (2016), as well as, by the wind-tunnel measurements by Ahmadi-Baloutaki et al. (2016). We should note, however, that this potential advantage still needs to be demonstrated by real-word operational VAWTs wind farms.

A number of studies in the literature have shown that dynamic stall phenomena and the large, coherent, structures generated are critical in defining the wake signature of VAWTs. Brochier et al. (1986), for example, used flow visualizations and laser Doppler velocimetry (LDV) to study the wake of a two-bladed VAWT at Reynolds number, $Re_D = 10,000$, (based on the free-stream velocity and the turbine diameter). They reported first and second order statistics at two different tip speed ratios (*TSRs*). They also found that at the lower *TSR*, dynamic stall caused the generation of leading and trailing edge vortices, populating the leeward side of the rotor. Higher values of Reynolds number, $\mathscr{O}(Re_D) = 10^5$, were considered in the PIV measurements by Simão Ferreira et al. (2009), at $TSRs = 2$, 3 and 4. It was confirmed that stall vortices were stronger at the lowest *TSR*, while at the highest *TSR* no vortex shedding was found. This was attributed to the decrease of the angle of attack experienced by each blade at the higher *TSR*. Earlier

---

[*] Corresponding author. CNR-INSEAN, Marine Technology Research Institute, Via di Vallerano 139, 00128 Rome, Italy.
E-mail addresses: antonio.posa@insean.cnr.it, aposa@gwu.edu (A. Posa), balaras@gwu.edu (E. Balaras).

https://doi.org/10.1016/j.jweia.2017.11.004
Received 26 June 2017; Received in revised form 3 November 2017; Accepted 5 November 2017

studies have also pointed to a strong wake asymmetry, which is associated to the different angles of attack seen by each airfoil on the leeward and windward sides of its trajectory, leading to asymmetry of vortex shedding. Bachant and Wosnik (2015), for example, utilized acoustic Doppler velocimetry to analyze the properties of the near wake of a VAWT ($Re_D = 10^6$ and $TSR = 1.9$). They measured higher turbulence levels on the leeward side of the wake, attributing them to stronger dynamic stall phenomena occurring on that side. Wake asymmetry was found also by Peng et al. (2016), who reported an experimental characterization of the wake of a five-bladed VAWT with a cambered airfoil ($Re_D \approx 2 \times 10^5$ and $TSR = 0.75$), providing details on the streamwise evolution of profiles of first and second order statistics, up to 10 diameters downstream. They conjectured that more vortices were shed on the windward side of the wake, although limitations of the resolution in space of probes measurements did not allow verification of such a hypothesis.

In addition to the experimental studies above, simulations have also contributed to our understanding of the wake structure in VAWTs. To date a number of studies based on the Reynolds-Averaged Navier-Stokes (RANS) approach have been reported (see, for instance, Hamada et al., 2008; Howell et al., 2010; Buchner et al., 2015; Giorgetti et al., 2015; Orlandi et al., 2015; Bremseth and Duraisamy, 2016; Zuo et al., 2016), as well as more sophisticated Detached Eddy Simulation (DES) analyses (Lei et al., 2017a, b). All the above strategies rely on turbulence models which require significant levels of semi-empirical input. In contrast, Large-Eddy Simulation (LES) resolves directly all the large, energetic, scales in the flow, while the small scales are parameterized using a subgrid scale (SGS) model. This feature makes LES more suitable to describe the behavior of the vortices associated to dynamic stall in VAWTs, albeit computationally more expensive. Some LES studies on VAWTs are already available in the literature (Li et al., 2013; Shamsoddin and Porté-Agel, 2014; Elkhoury et al., 2015). Li et al. (2013), for example, performed 2D URANS (Unsteady RANS) computations, as well as 3D URANS and LES, using periodic boundary conditions along the spanwise direction. They compared their results to experiments in the literature. Body fitted grids composed of about 130,000 and 5 million nodes were adopted for the 2D and 3D simulations, respectively. The Reynolds number was about $Re_D \approx 2 \times 10^6$ and the TSR varied between 0.7 and 1.96. They found improved predictions using LES, compared to URANS. They concluded that the main source of error for most of the URANS studies was due to the inability of RANS models to deal with flows experiencing significant stall phenomena. This conclusion was confirmed by Ouro and Stoesser (2017), who utilized a coupled LES/Immersed Boundary (IB) approach with local mesh refinement to simulate a vertical axis tidal turbine ($Re_D = 4 \times 10^5$ and $TSRs = 1.0, 1.5, 2.0, 2.5$ and 3.0). Their validation against experiments demonstrated better accuracy over RANS computations. Besides the above blade-resolving computations, LES studies coupled to an actuator line model (ALM) are available in the literature. In such case the effect of the blades on the flow is introduced by means a forcing function. Shamsoddin and Porté-Agel (2016), for example, utilized the ALM technique to study the wake of a VAWT in the atmospheric boundary layer using LES. They found a long wake recovery distance (14 diameters to reach 85% of the free-stream velocity), with the locations of maximum momentum deficit and turbulence intensity few diameters downstream of the rotor. An ALM approach, including a dynamic stall model (Mendoza et al., 2016), was also validated against experiments by Bachant et al. (2016), both in RANS and LES frameworks. A better agreement with reference datasets on wake flow was found in the latter case, even if a simple Smagorinsky model was adopted. Hezaveh et al. (2017) used a ALM-LES technique, where the SGS stresses were parameterized with the Lagrangian dynamic SGS model, to study the effects on the wake of VAWTs of the turbine aspect ratio, solidity and TSR. To improve the accuracy of the ALM model, coupled blade-resolving URANS computations were utilized to feed the ALM model with drag and lift coefficients. The study found that increasing the TSR resulted in a larger deficit in the wake, but also a faster wake recovery, due to stronger turbulent diffusion.

Although few LES studies were already reported, information on the coherent structures generated by blade stall and their effect on wake properties is still rather limited. This is primarily because it requires computationally expensive, high-fidelity simulations, where the turbine blades need to be directly resolved, rather than modeled. This is the focus of the present paper, where we report LES of an isolated VAWT using a conservative Cartesian solver, coupled with an IB methodology. Detailed validation of the computations by direct comparison of first and second order moments to PIV experiments have been presented in an earlier paper (Posa et al., 2016b). Here we expand our discussion of flow physics, focusing on the coherent structures produced by stall phenomena during both upwind and downwind trajectories of the airfoils. Their generation is correlated to the way TSR affects separation phenomena. The manuscript is organized as follows. The numerical method and computational setup are presented in Sec. 2. Results are discussed in Sec. 3. Conclusions are provided in Sec. 4.

2. Methodologies and setup

The filtered Navier-Stokes equations for incompressible flow are considered:

$$\begin{aligned} &\frac{\partial \tilde{u}_i}{\partial x_i} = 0 \\ &\frac{\partial \tilde{u}_i}{\partial t} + \frac{\partial \tilde{u}_i \tilde{u}_j}{\partial x_j} = -\frac{\partial \tilde{p}}{\partial x_i} - \frac{\partial \tau_{ij}}{\partial x_j} + \frac{1}{Re}\frac{\partial^2 \tilde{u}_i}{\partial x_j x_j} + f_i, \end{aligned} \tag{1}$$

where the operator, $\langle \sim \rangle$, indicates filtered quantities, indexes, i, and, j, denote the directions in space, u_i and x_i are the velocity component and coordinate along the direction i respectively, t is the time, p the pressure, Re the Reynolds number. In Eq. (1) f_i is a forcing term along the direction i. Note that the Reynolds number is defined as $Re = UL/\nu$, where U and L are the reference velocity and length scales, respectively, and ν is the fluid kinematic viscosity. The SGS tensor τ_{ij} is parameterized using the Filtered Structure Function model by Ducros et al. (1996). The deviatoric part of the SGS tensor is modeled by:

$$\tau_{ij} - \frac{1}{3}\tau_{kk} = -2\nu_t \tilde{S}_{ij}, \tag{2}$$

where ν_t is the eddy-viscosity, τ_{kk} the trace of the SGS tensor, and $\tilde{S}_{ij}$ the resolved strain rate tensor:

$$\tilde{S}_{ij} = \frac{1}{2}\left(\frac{\partial \tilde{u}_i}{\partial x_j} + \frac{\partial \tilde{u}_j}{\partial x_i}\right). \tag{3}$$

The eddy-viscosity, ν_t, is computed by:

$$\nu_t = 0.0014\, C_k^{-1.5}\, \Delta \sqrt{F_2^{(3)}}, \tag{4}$$

where C_k is the Kolmogorov constant, equal to 1.4, Δ the local filter size and $F_2^{(3)}$ the second-order structure function of the resolved velocity field, filtered 3 times by a high-pass Laplacian filter. The second-order structure function is defined as:

$$F_2 = \langle [\tilde{u}_i(\mathbf{x} + \mathbf{r}) - \tilde{u}_i(\mathbf{x})]^2 \rangle_{|\mathbf{r}|=\Delta}, \tag{5}$$

where the angular brackets stand for the spatial average in the region surrounding the point of coordinates $\mathbf{x}$ over a sphere of radius equal to Δ.

The geometry of the VAWT is immersed in a Cartesian grid and the boundary conditions on the rotating blades are enforced by means of the forcing term, f_i, using the IB formulation developed by Balaras (2004) and Yang and Balaras (2006). This approach relaxes the requirement for the mesh to conform to the body, and complex moving bodies can be